

Quantitative EPR study of Mn(II)salen oxidation within zeolite Y[†]

María. J. Sabater,¹ Avelino Corma,^{1*} Jose V. Folgado² and Hermenegildo García¹

¹Instituto de Tecnología Química UPV-CSIC, Universidad Politécnica de Valencia, Apartado 22012, 46071 Valencia, Spain

²Institut de Ciència dels Materials de la Universitat de Valencia, Dr. Moliner 50, 46100-Burjassot, Valencia, Spain

Received 11 February 1999; revised 26 October 1999; accepted 28 October 1999

ABSTRACT: Encapsulation of two different Mn(II)salen complexes within the supercavities of zeolite Y was accomplished by means of two established synthetic routes and they were unequivocally characterized by spectroscopic techniques [Fourier transform infrared, diffuse reflectance and electron paramagnetic resonance (EPR)]. In solution it is well established that high-spin Mn(II)salen complexes react spontaneously with molecular oxygen to yield various oxidation products. These include Mn(III) species and several oxy-bridged [Mn(salen)O]_n molecules. In the zeolite only the monomeric Mn(III)salen complex can be expected owing to the steric constraints imposed by these inorganic solids. This oxidation reaction from Mn(II) to Mn(III) was easily followed by EPR spectroscopy. According to these EPR measurements, the intrazeolitic oxidation of Mn(II)salen to Mn(III)salen by dioxygen proceeds with difficulty by virtue of a speculative lattice coordination stabilizing effect. This situation can be overcome by using efficient classical oxidants such as *tert*-butyl hydroperoxide or hypochlorite. Copyright © 2000 John Wiley & Sons, Ltd.

KEYWORDS: manganese(III); salen; electron paramagnetic resonance

INTRODUCTION

Alkene epoxidation is a versatile reaction in organic synthesis because the epoxide ring can readily be opened to produce 1,2 functionalities with almost complete regio- and stereocontrol. More recently, the process has gained an enormous importance in asymmetric synthesis because one or two neighboring chiral centers can be created with a high degree of enantioselectivity by means of powerful catalytic methods.^{1,2} Among them, chiral manganese–salen complexes have been found to be the most efficient enantioselective catalysts.^{3–5} Owing to the practical importance of this type of catalysts, much effort has been directed towards their immobilization on organic polymers and rigid inorganic matrices such as zeolites.^{6–9} Incorporation of the manganese–salen catalyst within microporous zeolites not only allows easy separation of the catalyst from the reaction mixture with the possibility of operating in a continuous manner, but more importantly decreases the tendency of the complex to undergo dimerization or autooxidation. This should lead to enhanced thermal stability and catalytic performance of

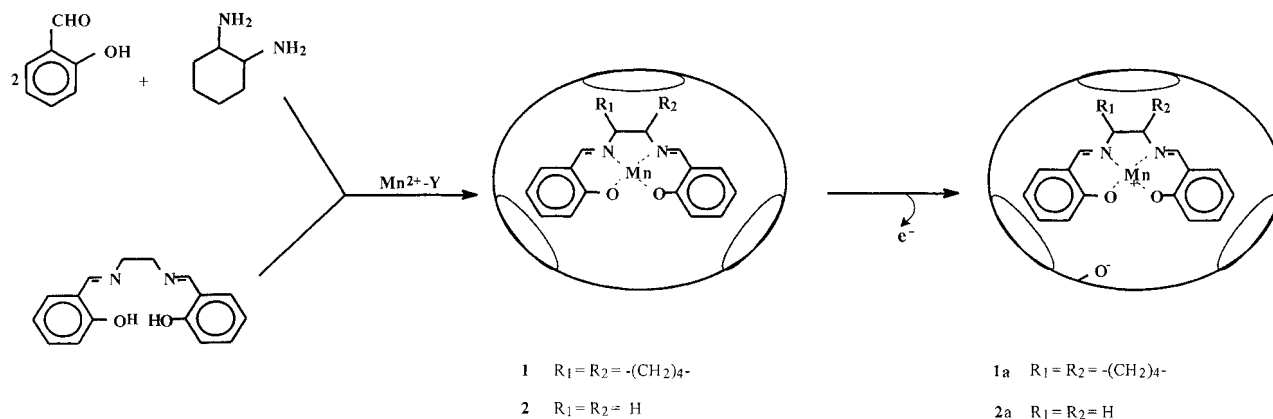
the complex. These materials, often denoted ‘ship-in-a-bottle’ complexes, have been prepared by different methodologies that in principle circumvent the manipulation of highly sensitive Mn(III) salts and rely on the use of molecular oxygen as oxidant to carry out the stoichiometric Mn(II)salen to Mn(III)salen conversion.^{6–9}

In solution, Mn(II)salen complexes are very prone to undergo oxidation to Mn(III)salen and also multiple oxy-bridged oligomeric and polymeric [Mn(salen)O]_n forms. In contrast, the Mn(II)salen complex has been found to be rather persistent in the interior of zeolite cavities. Aggregation to form [Mn(salen)O]_n is also effectively impeded within the cages.^{10–13} The use of zeolite Y-encapsulated Mn–salen complexes as epoxidation catalysts and their unprecedented stability in the interior of the zeolites make it necessary to assess the influence that different oxidation treatments have on the Mn(II)/Mn(III) oxidation state. For this purpose, two different manganese Schiff-base complexes (**1** and **2**) were synthesized within zeolite Y and characterized by a combination of spectroscopic techniques [Fourier transform infrared (FTIR), diffuse reflectance UV/Vis (DRS) and electron paramagnetic resonance (EPR)]. Among these methods, EPR and DRS were found to be sensitive to the oxidation state of the manganese atom and confirmed the initially predominant + II state of Mn. This allows us to follow in a quantitative manner the oxidation of Mn(II) to Mn(III) by different oxidizing reagents.

*Correspondence to: A. Corma, Instituto de Tecnología Química UPV-CSIC, Universidad Politécnica de Valencia, Apartado 22012, 46071 Valencia, Spain.

[†] Dedicated to Professor J. Elguero on the occasion of his 65th birthday.

Contract/grant sponsor: DGICYT; Contract/grant number: MAT97-1016-CO2.



Scheme 1. Preparation of manganese salen complexes in the supercages of zeolite Y

RESULTS AND DISCUSSION

The encapsulation of manganese Schiff-base complexes within zeolite Y was achieved according to previously described methods (Scheme 1).^{7,8,13} Encapsulated Mn(II)salchd [salchd = 1,2-bis(salicylideneimino)cyclohexane] complex (**1**) was prepared in a stepwise process requiring one diamine molecule (*cis*- and *trans*-1,2-cyclohexanediamine) and two molecules of salicylaldehyde

to diffuse into the Mn^{2+} pre-exchanged zeolite Y (0.47% Mn^{2+} , 1 Mn^{2+} every 5 supercages) to give the heterogenized complex **1** (Scheme 1). Exhaustive Soxhlet extraction with dichloromethane removed the excess of ligand and reactants from the inorganic solid while the bulky complex remained immobilized within the large supercavities (13 Å diameter) and could not diffuse through the smaller windows (7.4 Å). In addition to analytical measurements, the characterization of **1** was accomplished by DRS, IR and EPR spectroscopies.

Analogously, treatment of the Mn^{2+} -exchanged zeolite Y with the previously synthesized salen ligand [salen = 1,2-bis(salicylideneimino)ethylene] led to the formation of the heterogeneous complex Mn(II)salen (**2**). The yellow solid was Soxhlet extracted with dichloromethane to remove uncomplexed ligand. This flexible ligand, after binding the metal, forms a complex that is too large and rigid to escape through the 12-membered ring apertures of the cage and becomes immobilized inside the zeolite cavities (Scheme 1). The encapsulated complex **2** was characterized by its DR, IR and EPR spectra, which were very similar to those of complex **1** and were in complete agreement with the data reported in the literature.⁶

As can be seen in Fig. 1, the IR spectra of an authentic sample of homogeneous Mn(III)(salchd)Cl and heterogeneous Mn(II)salchd (**1**) and Mn(II)salen (**2**) complexes have in common the imine stretch vibration around 1615 cm^{-1} and the typical band of metallosalen complexes at 1540 cm^{-1} . Only insignificant minor shifts of the bands associated with ligand stretching modes could be measured, but these slight deviations ($<15\text{ cm}^{-1}$) are more likely to be caused by ligand distortion due to encapsulation in the solid supercage. In fact, data for the IR spectrum of Mn(II)salen reported in the literature for the most characteristic bands (1620 and 1525 cm^{-1}) are also very similar to those corresponding to complexes **1** and **2** (Fig. 1).¹⁴ Hence vibrational spectroscopy, which is probably the most widely applied analytical technique for the characterization of ship-in-a-bottle complexes, can-

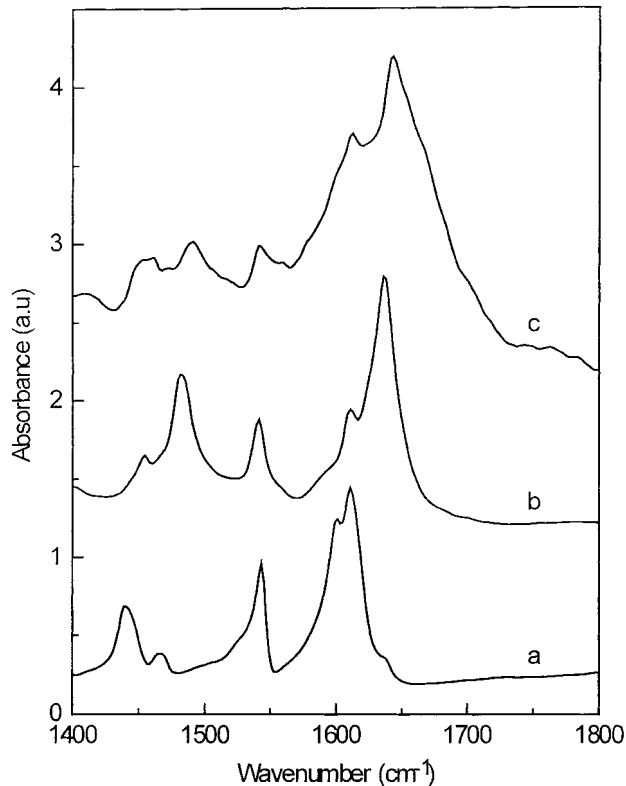


Figure 1. IR spectra of (a) Mn(III)(salchd)Cl (KBr) and heterogeneous complexes (b) **1** and (c) **2** incorporated inside zeolite Y. The IR spectra of the supported complexes were recorded at room temperature after heating at 200°C while outgassing at 10^{-5} mbar for 1 h

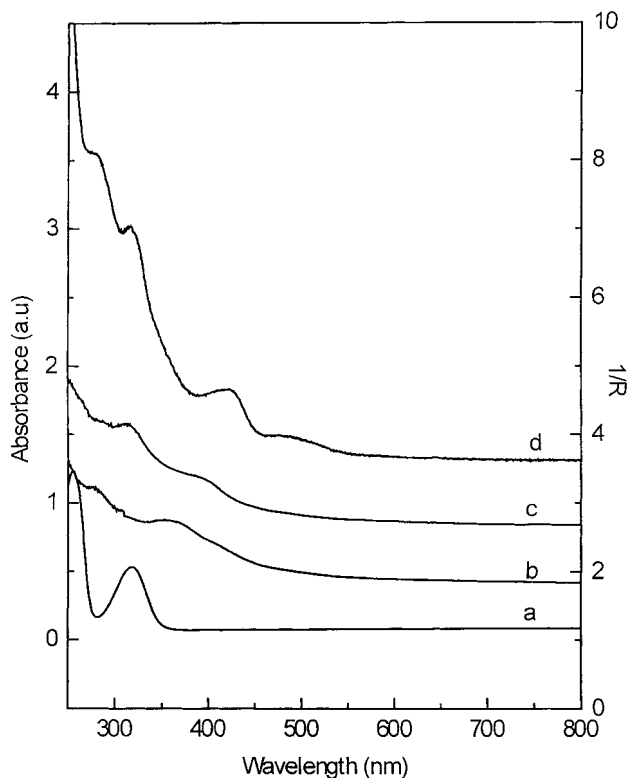


Figure 2. UV Vis spectra of (a) salen (10^{-4} M) in dichloromethane; DR spectra plotted as the inverse of the reflectance (R) of heterogeneous complexes (b) **1** and (c) **2** and (d) Mn(III)(salchd)Cl (10^{-4} M) in dichloromethane

not safely distinguish between the + II and + III oxidation states of the manganese.

By contrast, examination of the electronic absorption spectra in Fig. 2 shows some reliable differences between the spectra of Mn(II) and Mn(III) complexes. While **1**, **2** and the homogeneous Mn(III)(salchd)Cl sample have in common ligand transitions at 228, 255 and 318 nm, they differ in the characteristic weak d–d transition at about 500 nm typical of the brownish oxidized Mn(III)(-salchd)Cl that is absent in both complexes **1** and **2**. However, the low molar absorptivity of this absorption band does not allow one to take its presence as a valid criterion to assess the oxidation state of the manganese in the metallosalen complex incorporated in the zeolite. Moreover, quantification of the Mn(II)/Mn(III) ratio when metallosalen complexes having both oxidation states co-exist inside the zeolite voids would not be possible by this technique.

In contrast to IR and UV/Vis absorption spectroscopy, divalent and trivalent states of manganese can be easily differentiated by EPR spectroscopy. Mn(II) complexes show higher paramagnetism than that corresponding to the complexes of Mn(III). The intense spin–spin coupling of an even number of unpaired electrons combined with an extremely short relaxation time makes Mn(III) difficult to observe by EPR spectroscopy. Therefore,

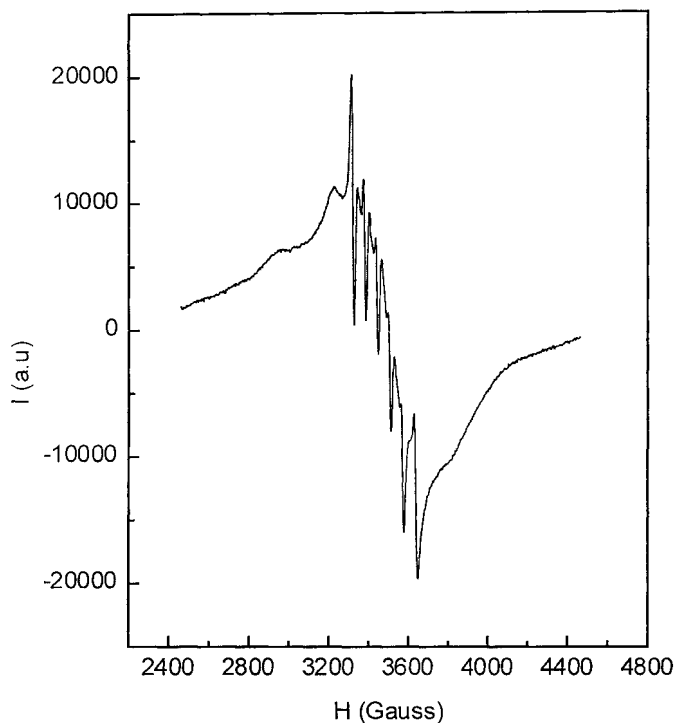


Figure 3. EPR spectra of heterogeneous complex **2** recorded at $t = 0$

EPR appears to be a suitable technique to determine quantitatively the Mn(II)/Mn(III) ratio of metallosalen complexes encapsulated inside zeolite Y. Isolated Mn²⁺ ions introduced into the zeolite show, upon complexation and formation of **1**, typical EPR spectra of high-spin Mn(II) ($S = 5/2$) with hyperfine couplings corresponding to an $I = 5/2$ nucleus and with negligible zero field splitting. The EPR signal observed around 3500 G has one set of six hyperfine lines that can probably be assigned to uncomplexed Mn(II) based on the similarity of the EPR spectrum with that of the original MnY without any ligand (Fig. 3).¹⁵ In addition to the sharp six-line pattern structure, there is also a much broader signal lacking fine structure showing visible shoulders separated more than 100 G underlying the fine structure. We propose that this broad signal corresponds to the Mn(II)salchd complex based on the comparison with MnY. Double integration shows that the amount of spins involved in the sharp six-line signal is negligible in comparison with that of the main broad line; so this sharp signal will not be considered further (Fig. 3).

When these EPR measurements were carried out with the initial ship-in-a-bottle salen complexes before submitting them to any oxidation treatment, quantification showed that within experimental error ($\pm 10\%$) all the manganese was in the + II oxidation state, as it was in the original Mn²⁺-exchanged zeolite Y. This agrees with the fact that the ion-exchange procedure of the commercial NaY was carried out using Mn(AcO)₂.

Table 1. Mn(III)/Mn(II) ratio treatment of encapsulated Mn-salen complexes with different oxidizing agents

Complex	Oxidant	Mn(II) (%) ^a		
		0h	1h	2h
1	O ₂	100	89	83
2	<i>t</i> -BuOOH	100	38	26
2	NaClO	100	35	24

^a Determined by double integration of the EPR spectra (estimated error $\pm 10\%$).

Quantification by EPR allowed us to follow conveniently the efficiency of two alternative oxidation procedures to transform Mn(II)salen into Mn(III)salen complexes when they are embedded inside zeolite micropores. It should be noted that this oxidation occurs very easily in solution. Hence the formation of heterogeneous Mn(III)salchd complex **1a** was first carried out by bubbling air through a stirred dichloromethane slurry of **1** at ambient temperature. The course of the oxidation was followed by recording EPR spectra at different reaction times. These spectra were very similar to the initial one shown in Fig. 3, with just a small decrease in the number of spins. A summary of the results is given in Table 1.

After 2 h of O₂ bubbling, the integration of the EPR signal showed that only 17% of the initial Mn(II) cations had been oxidized. The difficulty in carrying out the Mn(II)salen to Mn(III)salen oxidation inside the zeolite cavities sharply contrasts with the ease with which this process takes place in solution. Preliminary electrochemical measurements were unable to detect any Mn(IV) species in the zeolite (a report on the complete electrochemical study of the samples will be published separately). In contrast, it has been reported that the O₂ oxidation of unsupported Mn(II)salen complex gives a large variety of oxo dimers and other oxidized species.¹⁶

Mn-salen complexes encapsulated within Y zeolites have been used as heterogeneous catalysts for the epoxidation of alkenes using NaClO or organic hydroperoxides as oxidants.⁷⁻¹⁰ It can be anticipated that in this process, the first step would be a change in the Mn oxidation state from + II to + III to give rise the active Mn(III)salen complex, as would be the case in solution. In order to address this possibility and in view of the stability of **1** when entrapped inside the zeolite cavities, complex **2** was treated with a series of oxidants.

When H₂O₂ (35%) was slowly added to a yellow slurry of **2** in dichloromethane, rapid oxidative degradation of the complex took place, as revealed by the immediate discoloration of the solid, and further studies using H₂O₂ were not pursued. Fortunately *tert*-butyl hydroperoxide (*t*-BuOOH) behaved differently to H₂O₂ as oxidant and discoloration of complex **2** did not occur. The changes in the intensity of the EPR spectrum recorded after 1 h of reaction with *t*-BuOOH showed a drastic reduction in

spin count, in agreement with the transformation of Mn(II) into EPR-silent Mn(III). Double integration of the EPR signal showed that about 60% of the initial Mn(II) ions had been oxidized, leaving a residual Mn(II) signal with well resolved hyperfine structure. After 2 h an additional diminution of the initial Mn(II) population was measured (Table 1). Similar results were obtained using NaOCl as oxidant (see Table 1).

The population of residual Mn(II) atoms that do not undergo oxidation could be those inaccessible to *t*-BuOOH. One possibility would be that the fraction of non-oxidizable Mn(II) would correspond to that of uncomplexed metal cations located in sodalite cages. The possibility that the residual Mn(II) could be located in the supercages and derive from the oxidative degradation of the salen complex seems unlikely given that these salen complexes encapsulated within zeolites do not undergo fast deactivation when used as heterogeneous catalysts employing the same oxidizing reagents.

This reluctance shown by Mn(II)salen to undergo oxidation in the intracrystalline voids of faujasite Y by molecular oxygen compared with the ease of this process in solution has to be a direct consequence of the influence of the encapsulation. It could be that some of the framework oxygens of the zeolite intervene as extra ligands and stabilize the encapsulated Mn(II)salen complex. This possibility has been advanced previously for related complexes within zeolite Y.^{11,12}

In contrast, in solution when the 'high-spin' octahedral complex Mn(II)salen is chelated to suitable axial ligands such as Cl⁻, perturbation of the d orbitals promotes the change in the oxidation state from Mn(II) to Mn(III) by electron transfer to molecular oxygen, leading to the EPR-silent Mn(III)salenCl. If the axial ligand field of the coordinating ligand is not strong enough to accomplish this requirement, dioxygen could react in a different way, leading to another set of oxidized monomeric Mn(III) and oligomeric Mn(III)/Mn(IV) structures.

In zeolite Y, tetradentate salen ligands placed at equatorial positions and also lattice oxygens and/or hydration water are thought to account for the octahedral geometry of zeolite-occluded Mn(II) observed by EPR. It could be expected that upon oxidation monomeric Mn(III)salen complexes would be the only possible product since there is insufficient space for oligo- and polymerization. However, the observed difficulty in undergoing one-electron oxidation to Mn(III) can be taken as evidence in favor of an oxygen lattice coordination effect that would stabilize the d₅ electronic configuration of the encapsulated Mn(II)salen complex over the d₄ Mn(III)salen complex.

This exceptional coordinating role of zeolite Y has been invoked in numerous studies of heterogeneous transition metal complexes such as zeolite-encapsulated Mn(II)(bpy)_n, where it has also been pointed out that strong donor axial ligands could weaken the coordination of Mn(II) to the zeolite lattice.¹¹

Although EPR spectroscopy shows the oxidation of Mn(II) to silent Mn(III) species, complementary studies by IR spectroscopy of the final oxidized zeolite samples are necessary in order to assess whether or not Mn(III)salen has been formed. It was anticipated that the presence of adventitious reagent would complicate the IR spectrum of the resulting samples, but based on the data reported in the literature, the band at 1538 cm^{-1} can be taken as firm evidence of the presence of metallosalen complexes. This band was actually recorded at 1540 cm^{-1} and therefore it can be concluded that the oxidation of Mn(II)salen led to Mn(III)salen at least to some extent. However, this Mn(III)salen complex has been found to be very unstable and thermal treatment at 100°C and 10^{-2} Pa led to the complete disappearance of this characteristic band.

CONCLUSIONS

Synthesis of Mn(III) Schiff-base complexes **1a** and **2a** analogous to the original Jacobsen catalysts encaged in zeolite Y was accomplished by means of established preparation protocols and their structures were fully characterized by different spectroscopic techniques. The key oxidation step from Mn(II) to Mn(III) was carried out by oxygen and other traditional oxidants such as peroxides and commercial bleach and their efficiency was followed quantitatively by EPR spectroscopy.

In solution, the 'high-spin' octahedral complex Mn(II)salen is well known to undergo spontaneous oxidation to a complex set of products. These include Mn(III) species and oxy-bridged molecules represented by $[\text{Mn}(\text{salen})\text{O}]_n$. In the zeolite there is insufficient space in the supercages for oligomerization; hence monomeric Mn(III)salen complexes would be the only product expected.

According to EPR measurements, the intrazeolitic oxidation of Mn(II)salen to Mn(III)salen by molecular oxygen proceeds rather sluggishly by virtue of a speculative lattice coordination stabilizing effect. This situation can be overcome by employing a stronger oxidant such as those commonly used to effect alkene epoxidation.

EXPERIMENTAL

Compounds and materials. Starting reagents (salicylaldehyde, 1,2-cyclohexanediamine, etc.) and reagent-grade solvents were purchased from Aldrich and Scharlau, respectively, and were used without further purification.

1,2-Bis(salicylideneimino)ethylene ligand and the complex Mn(III)(salchd)Cl were prepared according to the procedures reported by Jacobsen for the *tert*-butyl analogs.¹⁷ Their purity was checked by comparing their spectra with the most characteristic spectroscopic data

(IR, FAB-MS) reported in the literature for the *tert*-butyl-substituted ligand and the Jacobsen catalyst.¹⁷

Zeolite Y was purchased from PQ Zeolites (specific surface area (BET, N_2) = $685.4412\text{ m}^2\text{ g}^{-1}$; $A_0 = 2.467\text{ nm}$; $\text{Na}_2\text{O} = 13.9\text{ wt\%}$; $\text{Si:Al} = 5.18$).

Oxidation procedures. (a) Oxidation by molecular oxygen was accomplished by bubbling air through a stirred suspension of 1.2 g of heterogeneous complex in 12 ml of dichloromethane; after oxidation, the solid was filtered off, washed exhaustively with dichloromethane and dried under a stream of N_2 .

(b) Oxidation with *t*-BuOOH was carried out by adding 0.5 ml of the hydroperoxide to a stirred suspension of 1.2 g of heterogeneous complex in 5 ml of dichloromethane; after oxidation, the solid was filtered off, washed with dichloromethane and dried under a stream of N_2 .

(c) Oxidation with NaClO was carried out by adding 3 ml of NaClO (4%) to a stirred suspension of 1.2 g of the complex embedded within zeolite in 5 ml of dichloromethane; after oxidation, the solid was filtered off, washed with water and dried under a stream of N_2 .

EPR spectra. Room temperature EPR spectra were recorded on a Bruker ER200D spectrometer, working at the X-band (9.65 GHz) and using DPPH ($g = 2.0036$) as standard reference.

IR spectra. FTIR spectra of the complexes in zeolites were recorded at room temperature using a greaseless CaF_2 cell in a Nicolet 710 FT spectrophotometer. Self-supported wafers ($\sim 10\text{ mg}$) were prepared by compressing the zeolite powder at 1 cm^{-2} . The samples were outgassed at 100°C and 10^{-2} Pa for 1 h before recording the IR spectra.

UV/Vis spectra. Room temperature transmission UV/Vis spectra were recorded with a Shimadzu UV/Vis scanning spectrophotometer. DR spectra of the opaque powders, plotted as the inverse of the reflectance, were recorded with a Varian Cary 5G UV/Vis NIR spectrophotometer.

Acknowledgements

Financial support by the Spanish DGICYT (H.G., MAT97-1016-CO2) is acknowledged. M.J.S. thanks the DGICYT for a reincorporation fellowship.

REFERENCES

1. Johnson RA, Sharpless KB. In *Comprehensive Organic Synthesis*, Vol. 7, Trost BM, Fleming I (eds). Pergamon Press: Oxford, 1991; Ch. 3.2, 389–436.
2. Johnson RA, Sharpless KB. In *Catalytic Asymmetric Synthesis*, Ojima I (ed). VCH: New York, 1993; Ch. 4.1, 101–158.

3. Zhang W, Loebach JL, Wilson SR, Jacobsen EN. *J. Am. Chem. Soc.* 1990; **112**: 2801.
4. Chang S, Galvin JM, Jacobsen EN. *J. Am. Chem. Soc.* 1994; **116**: 6937.
5. Irie R, Noda K, Ito Y, Matsumoto N, Katsuki T. *Tetrahedron Lett.* 1990; 7345.
6. (a) Bowers C, Dutta PK. *J. Catal.* 1990; **122**: 271; (b) Balkus KJ, Gabrielov AG. *J. Inklus Phenom. Mol. Recog. Chem.* 1995; **21**: 159.
7. Ogunwumi SB, Bein T. *Chem. Commun.* 1997; 901.
8. Sabater MJ, Corma A, Domenech A, Fornés V, García H. *Chem. Commun.* 1997; 1285.
9. Minutolo F, Pini D, Salvadori P. *Tetrahedron Lett.* 1996; **37**: 3375.
10. Varkey SP, Ratnasamy C, Ratnasamy P. *J. Mol. Catal.* 1998; **135**: 295.
11. Knops-Gerrits PP, De Vos D, Thibault-Starzyk F, Jacobs PA. *Nature (London)* 1994; **369**: 543.
12. Alvaro M, Fornés V, García S, García H, Scaiano JC. *J. Phys. Chem. B* 1998; **102**: 8744.
13. Sabater MJ, García S, Alvaro M, García H, Scaiano JC. *J. Am. Chem. Soc.* 1998; **122**: 8521.
14. Srinivasan K, Michaud P, Kochi JK. *J. Am. Chem. Soc.* 1986; **108**: 2309.
15. (a) Zawacki M, Gutsze A, Komagotowski J. *Bull. Soc. Chim. Belg.* 1990; **99**: 561; (b) De Vos D, Bein T. *J. Am. Chem. Soc.* **119**: 9460.
16. Matsushita T, Yarino T, Masuda I, Shono T, Shinra K. *Bull. Chem. Soc. Jpn.* 1973; **46**: 1712.
17. Larrow JF, Jacobsen EN. *J. Org. Chem.* 1994; **59**: 1939.